

Supporting Information

Bereiter et al. 10.1073/pnas.1204069109

SI Text

SI Materials and Methods. Synchronization of CO₂ records. For temporal comparability, we synchronized the data of the Byrd and TALDICE cores to the EDML1 Scenario 4 gas age scale (1) by matching the tie points (Fig. 1) in the CH₄ records of the different ice cores, based on the work of ref. 2. Between the tie points, the age scales for Byrd and TALDICE have been linearly interpolated. We used the same principle for the Taylor Dome data (3) but in an indirect way. Here, we translated the age scale of ref. 4, for which a synchronization with Taylor Dome data exists. This indirect synchronization is less suitable for our purposes for two reasons: First, we do not know the uncertainties of the synchronization between the Byrd and Taylor Dome data; second, CO₂ matching has been partly applied in that synchronization, which is less precise due to the rather slow atmospheric CO₂ changes. To better identify the tie points in the TALDICE record around DO 17 to 14, we used new highly resolved CH₄ data measured with a continuous flow analysis technique (5). Tie points are identified where rapid CH₄ changes occur and their location is thus not dependent on the absolute values of CH₄, which may differ in ref. 5 from those in ref. 2. If possible, we matched the midpoints of the CH₄ change, otherwise maxima associated with DO-events are used.

Offsets between CO₂ records. Several issues have to be taken into account when comparing CO₂ records from different ice cores and measured in different labs:

- i. Different analytical methods and independent standardization can lead to interlaboratory offsets. Moreover, non-linearities in the standardization may lead to offsets that can depend on the mean CO₂ concentration, if those non-linearities are not corrected.
- ii. The ice core gas records are given on age scales that are CH₄ synchronized using best practice approaches; however, smaller synchronization errors on the order of a few centuries may still exist, especially for time periods where no synchronization tie points exist. This may lead to offsets in concentrations away from intervals of stable CO₂ levels and away from tie points.
- iii. The different enclosure characteristics of various ice cores lead to a different damping of fast CO₂ changes. Thus, a direct comparison of CO₂ levels from different ice cores is only unambiguous for CO₂ changes that last significantly longer than the width of the age distribution of the air bubbles in the ice. In the cores used here, this width is on the order of a few centuries, with Taylor Dome having the widest and Byrd the narrowest glacial age distribution. Accordingly, the amplitude of changes in maxima and minima can be different in ice cores if concentration variations are short-lived. Another effect related to the firnification process is gravitational enrichment of CO₂ relative to N₂. This effect leads to an enrichment on the order of 1–2 ppmv at the bubble close-off depth. The size of this effect depends on the depth of the diffusive firn column at the different sites. Accordingly, we estimate this effect to explain offsets between individual cores of maximum 1 ppmv. Also atmospheric CO₂ concentration changes could lead to a diffusive enrichment/depletion, if the firn column is not in CO₂ equilibrium with the atmosphere. The CO₂ changes observed in our records, however, are too slow for this to be the case.
- iv. A clear fractionation between CO₂ and the main air components has been observed in the bubble clathrate transition zone (BCTZ) (6). Here, CO₂ is preferentially included into clathrates, leading to an enrichment in the integrated clathrate CO₂ content and a depletion in the remaining integrated bubble content. Due to the incomplete extraction efficiency of dry extraction techniques, the air enclosed in remaining bubbles is preferentially released. Thus, techniques with different extraction efficiencies lead to offsets in the CO₂ concentration for BCTZ ice and high scatter in the data (6). Here, we used only ice well below the BCTZ to minimize the bubble/clathrate fractionation problem. Moreover, large clathrates are formed later in the clathrate formation process (i.e., deep in the BCTZ) than smaller ones (7). Also the CO₂ content in clathrates is expected to be highest in (small) clathrates formed at the top of the BCTZ and decrease with depth as is the case for the O₂/N₂ ratio (7). Thus, the CO₂ content in clathrates might be different within the BCTZ. Below the BCTZ, diffusion in the ice slowly re-equilibrates the clathrates (6). This process, however, requires several millennia. Accordingly, preferential extraction of gas entrapped in large clathrates just below the BCTZ using dry extraction techniques can lead to a similar albeit smaller depletion in CO₂ concentration, as is the case in mixed bubble/clathrate ice from the BCTZ.
- v. The storage time for different ice cores differs. For example, the Byrd ice core has been stored in cold rooms at only –20 °C for nearly 40 y before the analyses performed (4). In this time, many clathrates relax back to bubbles, during which a fractionation of gases may occur again. In summary, offsets between different ice core measurements may also be due to a different stage of the clathrate relaxation process. Based on our observations of CO₂ enrichment in clathrates in the BCTZ, we would expect the reverse fractionation to occur during this relaxation. Accordingly, the integrated CO₂ content should be depleted in the reformed bubbles. The more complete the relaxation process is, the less depleted the integrated bubble content should become in CO₂. However, also net gas loss has been observed in ice stored at higher temperatures (8). This would lead to a net enrichment of the CO₂ concentration in the ice, which becomes stronger the more O₂ is lost from the ice. Careful sample selection away from the outer surface of the ice core (where loss processes play the strongest role), as done in our analyses, helps to minimize this effect (9).
- vi. Finally, also in situ CO₂ production by oxidation of organic acids and carbonate-acid reaction, as notoriously observed in Greenland ice (10, 11), can also not be ruled out entirely for Antarctica. This effect is estimated to be smaller than 1.5 ppmv for Antarctic ice (9).

Given this long list of processes that can influence the CO₂ concentration in Antarctic ice cores, it is not surprising to observe differences between different labs and ice cores of a few ppmv. Fig. 1 in the main text shows that the different records agree in the temporal changes in CO₂, but not in the mean level of CO₂ concentrations. Moreover, these offsets are not always constant over the entire records.

In the following, we concentrate on a few features in these offsets and provide potential explanations. Note however, that the relative temporal changes in CO₂ discussed in the main text are seen in all records and, thus, the small offsets do not affect our conclusions drawn on the phasing between DO event onsets and CO₂.

(Table S1). Based on these six values, an average rate of change before a CDM of 6.1 ± 0.6 ppmv/kyr for MIS 3, and 14.6 ± 3.7 ppmv/kyr for MIS 5 is found. On the one hand, the values of CDM 19 and 23 are excluded and, hence, the validity of the MIS 5 value can be challenged. On the other hand, if all events during MIS 5 are included the average rate of change is at 12.2 ± 2.8 ppmv/kyr and the four highest rates of change are found during MIS 5 (Table S1). Based on these results, it appears that rates of change before CDM are larger for MIS 5 than for MIS 3.

Significance test of the difference in the CDM delay between MIS 3 and MIS 5.

To determine the statistical significance of the different delays of CDM relative to the DO onsets between MIS 3 and MIS 5, the null hypothesis that the delay of CDM relative to the DO onset is equal for MIS 3 and MIS 5 was tested against the hypothesis that this delay is greater during MIS 3 than MIS 5 using a conservative strategy. For each CDM, the delay relative to the DO onset and its uncertainty was determined based on the Monte Carlo splines with 500 y cut-off period (Table S2). To the uncertainty of the delay derived from the splines, the maximum uncertainty in the onset of the DO-event trigger was added (defined by the time interval between the two CH₄ data points defining the onset, Fig. S1). Note that this is a conservative estimate, since the uncertainty of the delay and of the DO onset trigger are independent of each other. This defines a new delay uncertainty for each event in MIS 3 and MIS 5 shown in Fig. 2 (top boxes) and Table S2. Using these new uncertainties, a Monte Carlo simulation was performed producing 1,500 possible values for each event. The mean and the standard deviation over all values for the MIS 3 and MIS 5 period, respectively, were calculated and tested in an independent two-sample *t*-test.

A first conservative approach is to use only results based on the EDML record since it is the only record that covers all events

and, hence, all delays originate from the same ice core. This approach results in a *t*-value of 1.85 which is slightly lower than the critical *t*-value for a one-sided test with 6 degrees of freedom and 95% significance (1.94) and higher than the one for 90% significance (1.44). However, a Wilcoxon rank sum test (or Mann-Whitney U test) using the means of each CDM shows a significance above 95%.

The EDML record has two weaknesses which influence the delay for MIS 5 CDM using this splining strategy: First, the resolution of CDM 24 is rather coarse for the 500 y cut-off period spline. Second, CDM 23 has both an exceptional large uncertainty (see Fig. 2) due to the smaller amplitude and a DO trigger that can be questioned (Fig. S1). When CDM 24 from the EDC record (18) is added—no matter if we include CDM 23 or not—the rank sum tests show a clear significance above 95%. This is also true for the *t*-test when CDM 24 is included but CDM 23 excluded. If both CDM are included, the significance is just around 95%.

So far, no data from the TALDICE ice core has been taken into consideration for these significance tests. Due to the higher quality of the TALDICE records, the delay estimates of the MIS 3 type events are more precise as the ones derived from the EDML records. In a last step, the estimates from the TALDICE records are used as additional independent measures of the delay of MIS 3 type events. Using the TALDICE delays, the significance is above 97.5% (*t*-value = 2.50; critical *t*-value for 97.5% significance and 10 degrees of freedom = 2.23).

In summary, this means that CDM of MIS 3 show a larger delay relative to their corresponding DO event onsets than CDM of MIS 5 with a significance around 95%, using EDML data only. However, the estimates derived from the EDC and TALDICE records can be used as independent measure of the delay of MIS 3 and MIS 5 type events increasing the significance above 97.5%.

- Loulergue L, et al. (2007) New constraints on the gas age-ice age difference along the EPICA ice cores, 0–50 kyr. *Clim Past* 3:527–540.
- Schilt A, et al. (2010) Atmospheric nitrous oxide during the last 140,000 years. *Earth Planet Sci Lett* 300:33–43.
- Indermühle A, Monnin E, Stauffer B, Stocker TF, Wahlen M (2000) Atmospheric CO₂ concentration from 60 to 20 kyr BP from the Taylor Dome ice core, Antarctica. *Geophys Res Lett* 27:735–738.
- Ahn J, Brook EJ (2008) Atmospheric CO₂ and climate on millennial time scales during the last glacial period. *Science* 322:83–85.
- Schüpbach S, Federer U, Bigler M, Fischer H, Stocker TF (2011) A refined TALDICE-1a age scale from 55 to 112 ka before present for the Talos Dome ice core based on high-resolution methane measurements. *Clim Past* 7:1–16.
- Lüthi D, et al. (2010) CO₂ and O₂/N₂ variations in and just below the bubble-clathrate transformation zone of Antarctic ice cores. *Earth Planet Sci Lett* 297:226–233.
- Salamatin AN, Lipenkov VY, Ikeda-Fukazawa T, Hondoh T (2001) Kinetics of air-hydrate nucleation in polar ice sheets. *J Cryst Growth* 223:285–305.
- Bender ML (2002) Orbital tuning chronology for the Vostok climate record supported by trapped gas composition. *Earth Planet Sci Lett* 204:275–289.
- Bereiter B, Schwander J, Lüthi D, Stocker TF (2009) Change in CO₂ concentration and O₂/N₂ ratio in ice cores due to molecular diffusion. *Geophys Res Lett* 36:1–5; AGU doiidentifier: L05703 doi: 10.1029/2008GL036737.
- Anklin M, Barnola J, Schwander J, Stauffer B, Raynaud D (1995) Processes affecting the CO₂ concentrations measured in Greenland ice. *Tellus* 47B:461–470.
- Smith HJ, Wahlen M, Mastroianni D (1997) The CO₂ concentration of air trapped in GISP2 ice from the last glacial maximum-holocene transition. *Geophys Res Lett* 24:1–4.
- Neffel A, Oeschger H, Staffelbach T, Stauffer B (1988) CO₂ record in the Byrd ice core 50,000–5,000 years BP. *Nature* 331:609–611.
- Huber C, et al. (2006) Isotope calibrated greenland temperature record over marine isotope stage 3 and its relation to CH₄. *Earth Planet Sci Lett* 243:504–519.
- Spahni R, et al. (2003) The attenuation of fast atmospheric CH₄ variations recorded in polar ice cores. *Geophys Res Lett* 30:1–4; AGU identifier: 1571 doi: 10.1029/2003GL017093.
- Ruth U, et al. (2007) “EDML1”: A chronology for the EPICA deep ice core from Dronning Maud Land, Antarctica, over the last 150,000 years. *Clim Past* 3:475–484.
- Buiron D, et al. (2011) TALDICE-1 age scale of the Talos Dome deep ice core, East Antarctica. *Clim Past* 7:1–16.
- Enting IG (1987) On the use of smoothing splines to filter CO₂ data. *J Geophys Res* 92:10977–10984.
- Schneider R (2011) Quantifying past changes of the global carbon cycle based on δ¹³C₂ measurements in Antarctic ice cores. PhD thesis (Univ of Bern).

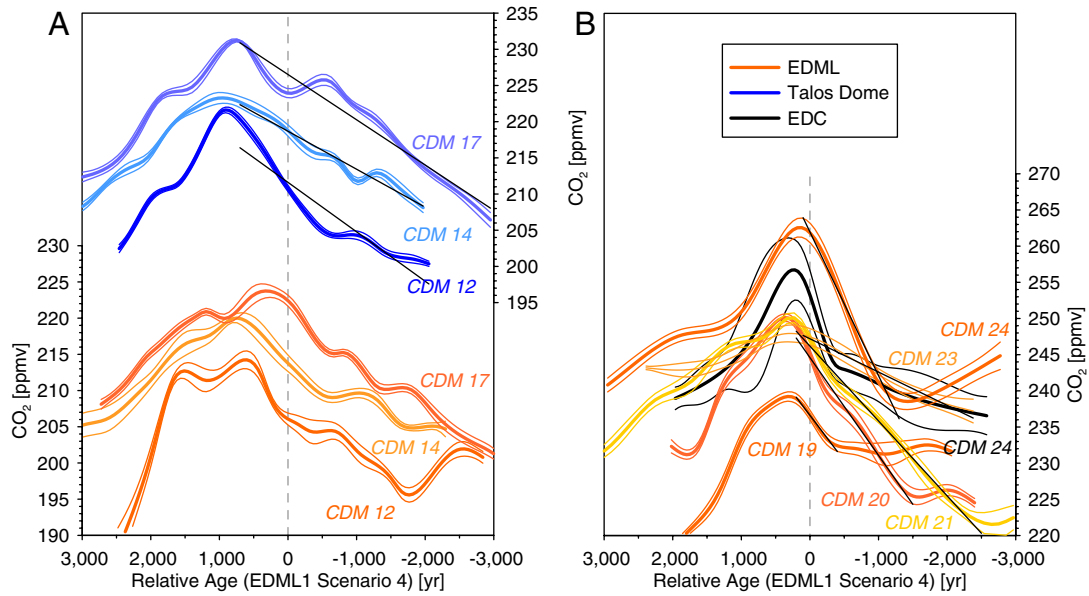


Fig. S3. Splines through CDM with 1,000 y cut-off period. Line, color, and axis affiliations are equal to Fig. S2. Black lines show linear regressions of the corresponding average splines. For the calculation of the regression, the period for which the black lines are plotted has been used. Slopes of the regressions are given in Table S1.

Table S1. Results or linearly interpolated rates of change prior to the peak of the CDM. Values for CDM 12, 14, and 17 are based on TALDICE records; values for CDM 19, 20, 21, 23, and 24 are based in EDML records. The window of linear interpolation is indicated by the black line in Fig. S3

CDM Nr.	12	14	17	19	20	21	23	24
Rates of change [ppmv/kyr]	6.8	5.2	6.3	(12.5)	13.5	10.3	(4.6)	19.9

Table S2. Calculated mean delays of CDM with respect to their corresponding DO event and associated errors (units = years) (Fig. 2)

	CDM Nr.	12	14	17	19	20	21	23	24
EDML	Mean	599	856	540	270	328	251	325	145
	error (σ)	252	387	334	157	160	140	486	172
TALDICE	Mean	927	943	737	-	-	-	-	-
	error (σ)	91	155	87	-	-	-	-	-
EDC	Mean	-	-	-	-	-	-	-	269
	error (σ)	-	-	-	-	-	-	-	327